

THE DEVELOPMENT AND APPLICATION OF A PHOTOEMISSION MODEL FOR CESIATED PHOTOCATHODE SURFACES

K. L. Jensen, J. E. Yater, J. L. Shaw, Naval Research Laboratory, Washington DC, 20375 USA
N. A. Moody, D. W. Feldman, P. G. O'Shea, University of Maryland, MD 20742, U.S.A.

Abstract

A theoretical photoemission model including thermal and field effects is presented. Particular attention is given to considering the impact of electron-electron and electron-lattice scattering and the development of an integrated absorption-transport-emission model developed to evaluate the moments of the electron emission distribution function. For the experimental conditions to which the theory is compared, there are no adjustable parameters. The performance of the model for the QE of bare metals and coated surfaces is discussed. A simple asymptotic model of emittance and brightness is given.¹

INTRODUCTION

A high quantum efficiency (QE) photoemitter capable of in situ rejuvenation would fill a critical need in the development of high power FELs and linear accelerators. The demands placed on photocathode and drive-laser combinations by high power FELs are often both demanding and conflicting. Nano-Coulomb bunches in O(10) ps time scales require high quantum efficiency photocathodes, but such cathodes have traditionally degraded prematurely in vacuums characteristic of rf photoinjectors, whereas more rugged metal photocathodes require short wavelengths and therefore demand much of the drive lasers. The dispenser photocathode is intended to provide a rugged, low work function, long lived photocathode addressing these conflicting needs, and its development necessitated a validated photocathode model capable of analyzing data and predicting performance. A program to develop a controlled porosity dispenser (CPD) photocathode led to the creation and validation of a theoretical model that accounts for low work function surfaces from submonolayer coverage of alkali (and alkali earth) metals [i]. Efforts to extend and update that model have been in response to two needs: first, to provide theoretical support to an experimental CPD photocathode program by systematically studying cesiated surfaces, conventional sintered tungsten dispenser cathodes, and ultimately, custom engineered dispenser cathode; and second, to render the validated photoemission model in a form amenable to particle-in-cell (PIC) beam simulation codes [ii, iii] to predict performance of an rf injector gun using such a photocathode. Here the latest modifications to the model and its application are discussed.

Changes to the theoretical model are on two fronts. First, the scattering model affecting photoelectron excited transport to the surface has been revised. Second, the revisions motivated a moments-based emission model that is able to address cathode emittance. The beams of

high power FEL's will be space charge dominated at some stage in the accelerator but especially in the gun. Non-uniform, transverse and temporal distributions affect emittance, and while the problem is of significant concern, predictive modeling efforts of device operation are compromised by the lack of adequate emission models in beam simulation codes. The photoemission models developed attempt to rectify the deficiency.

THE PHOTOEMISSION MODEL

Background

The photoemission model described in Ref. [i] represented quantum efficiency QE by

$$QE(T, F) = \frac{q}{h\omega} F_\lambda(T)(1-R)P(h\omega) \quad [1]$$

$$P(h\omega) = \frac{U[\beta_T(h\omega - \phi)]}{U[\beta_T\mu]}$$

where $R(\omega)$ is the reflectivity of the surface, P is a probability of emission factor, U is the Fowler-Dubridge function, $\beta_T = 1/k_B T$ is the inverse temperature, ϕ is the barrier height above the Fermi level (work function minus Schottky barrier lowering factor, or $\Phi - \sqrt{4QF}$, where $Q = 0.36$ eV-nm and F is the product of electric field and electron charge). When coatings such as Cs are introduced, the work function Φ is dependent upon the degree of coverage θ in a manner predicted by Gyftopoulos-Levine theory. The scattering factor F_λ (not to be confused with field F) governs the probability that an electron will suffer a scattering event on its trajectory towards the surface and therefore be prevented from being photoemitted. It can be approximated by

$$F_\lambda \approx \frac{1}{\pi} \int_0^{\pi/2} \frac{\cos(\theta)}{\cos(\theta) + (\delta/l(E))} d\theta \quad [2]$$

where δ is the laser penetration depth, and the length $l(E)$ is the product of the electron velocity and relaxation time (the notation has changed from Ref. [i])

Amending recent work in measuring the QE of cesiated surfaces and the prediction of the QE of bare metals, we have revised components of the QE model by first, utilizing models of the relaxation rates τ implicit in f_λ at the electron energy augmented by the photon energy, and second, using a moments-based approach that changes the probability of emission term P . It is the moments-based approach that allows for transverse energy and velocity expectation values to be determined, from which estimates of the emittance and brightness can be made.

¹ Support by Joint Technology Office & Office of Naval Research

Scattering Rates and Their Determination

The relaxation time is taken to be the sum of three components:

$$\tau^{-1} = \tau_{ee}^{-1} + \tau_{ac}^{-1} + \tau_{imp}^{-1} \quad [3]$$

where “*ee*” refers to electron-electron, “*ac*” refers to acoustic phonon, and “*imp*” to residual low temperature scattering due to impurities or defects. In the case of electron-electron scattering, the scattering rate is given by

$$\tau_{ee} = \frac{4\hbar K_s^2}{\alpha^2 \pi m c^2 (k_B T)^2} \left[\left(1 + \frac{E - \mu}{\pi k_B T} \right) \gamma \left(\frac{2k_F}{q_o} \right) \right]^{-1} \quad [4]$$

$$\gamma(x) = \frac{x^3}{4} \left(\tan^{-1} x + \frac{x}{1+x^2} - \frac{\tan^{-1} \left(x\sqrt{2+x^2} \right)}{\sqrt{2+x^2}} \right)$$

where K_s is the dielectric constant, α is the fine structure constant, k_F is the Fermi wave vector, and q_o is the Thomas-Fermi screening length [iv] (the form given here corrects coefficient errors that exist in Ref. [iv]). To leading order, the Thomas-Fermi factor is given by

$$q_o^2 = \frac{4\alpha m c}{\pi \hbar^2 K_s} \sqrt{2m\mu} \quad [5]$$

For acoustic scattering, the rate is given by [v]

$$\tau_{ac} = \frac{\pi \rho \hbar^3 v_s^2 (T_D / T)^5}{m k_B T k_F \Xi^2} \left(\int_0^{T_D/T} \frac{s^5 ds}{(e^s - 1)(1 - e^{-s})} \right)^{-1} \quad [6]$$

where Ξ is the magnitude of the deformation potential, T_D is the Debye temperature, v_s is the velocity of sound, and ρ is the density. The Debye Temperature is given by

$$T_D = \frac{\hbar v_s}{k_B} (6\pi^2 N r)^{1/3} \quad [7]$$

where N [# / cm³] is the number density of the crystal, r is the (# of atoms / unit cell), and v_s is the sound velocity.

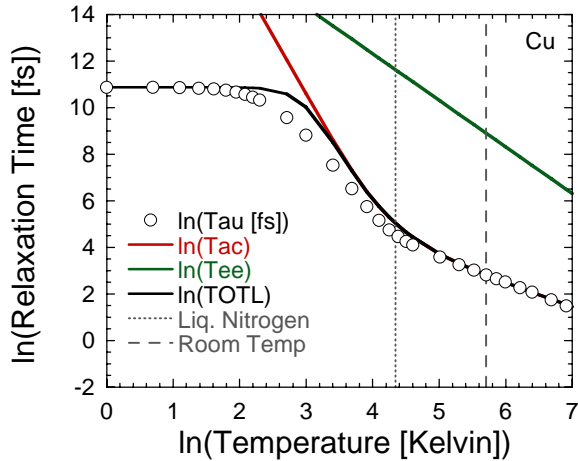


Figure 1: Determination of τ_{imp} and Ξ from thermal conductivity data from the literature.

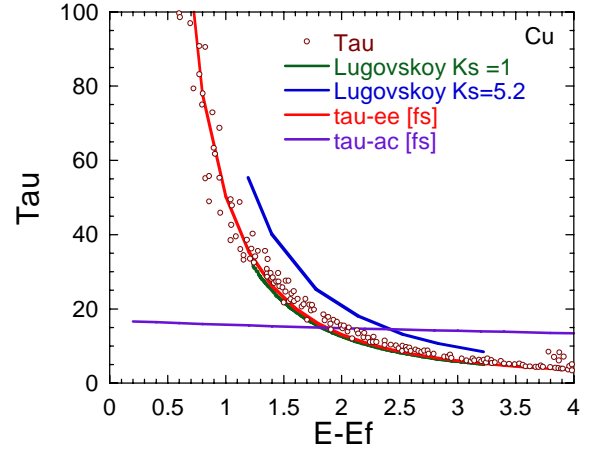


Figure 2: Determination of K_s from Monte Carlo simulations (red line) compared to parameters considered by Lugovskoy and Bray (green and blue)

Consequently, three parameters require an intricate simultaneous determination: τ_{imp} , K_s and Ξ . The values of τ_{imp} and Ξ are determined by low temperature thermal conductivity measurements after K_s is determined from Monte Carlo simulations in the literature [vi].

Comparison to Experiment

An example for Cu is shown in Figure 1 and 2. The procedure is reiterated for many metals, and in particular, for tungsten (W) and silver (Ag) which are the two cesiated metals experimentally examined [vii]. Parameters extracted from the literature become part of a library of material terms implicit in code and are not adjusted further. Comparisons of predictions of the resulting model with experimental data have been favorable for the cases of photoemission from copper [viii] and lead [ix] for a range of photon frequencies, as well as for other metals and particular frequencies discussed in the literature.

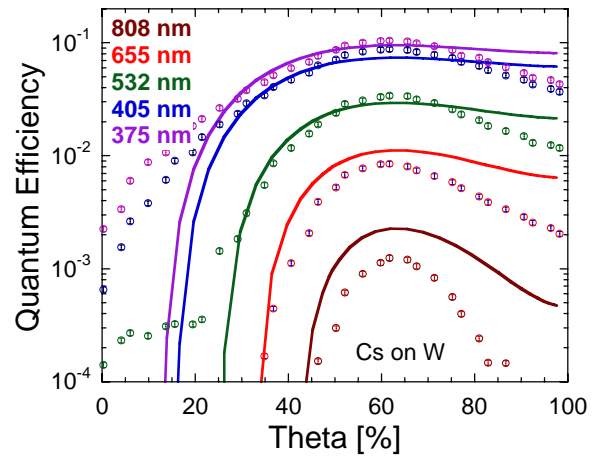


Figure 3: QE of Cs on W for low F and I_λ at 300 K versus fractional surface coverage (Ar-cleaned W). Symbols = experimental data; lines = theoretical model.

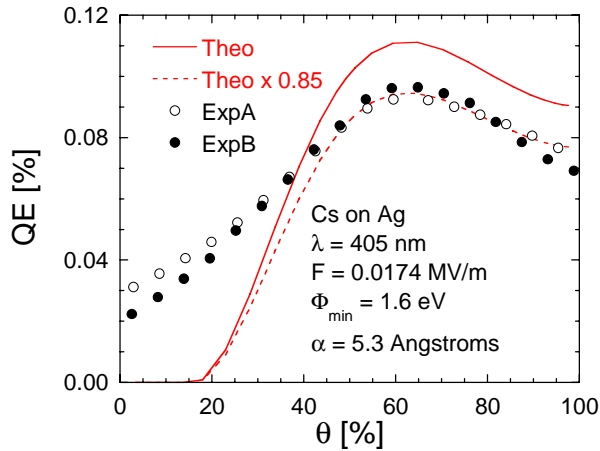


Figure 4: QE of Cs on Ag for conditions as in Fig. 3

Using the Gyftopoulos-Levine theory to relate the degree of surface coverage of Cesium on a bulk metal to the resulting work function [i], the prediction of QE for Cs on W and Cs on Ag was made and compared to experimental data. The results of that comparison are shown in Figures 3 and 4, respectively. The low coverage discrepancy shown in Fig. 4 is due to residual Cs on the surface from one experiment to the other. Issues of surface contamination led to investigations of cleaning using Ar ions, resulting in the better results for Cs on W shown in Fig. 3.

Origin Of Experimental-Theoretical Differences

The overall comparison between theory and experiment is shown to be remarkably good. Nevertheless, there are differences and an account of their probable origins is necessary. Theoretically, a simple nearly-free electron gas model is presumed, and so the significant complexities introduced by the density of states near the Fermi level are suppressed, and such complexities can matter for transition metals. Experimentally, in contrast to physical surfaces, the theoretical models are highly idealized. Cleaning is required to remove contaminants, and if due to sputtering, structure can be introduced. If the cathode is heated for cleaning, not all metals endure the necessary temperatures because of relatively low melting points (W can be strongly heated, whereas Ag cannot). Residual contamination can therefore remain in addition to what collects from an imperfect vacuum. Adsorbates often have higher work functions, e.g., carbon-based contamination can induce local work functions of 5.5 eV. Assuming the surface is adequately cleaned, different exposed crystal faces can show markedly different work functions (e.g., faces of Cu can vary by almost 0.8 eV): moreover, in Gyftopoulos-Levine theory, the exposed crystal plane affects the *f*-factor (see Ref. [i]: affects the number of Cs atoms per unit area) and which changes the shape of the QE hump: observations of the tungsten face, as shown in Figure 5, as well as considering other values of *f* suggest the generic (single) value chosen for *f* is not necessarily the optimal value when several faces are present.

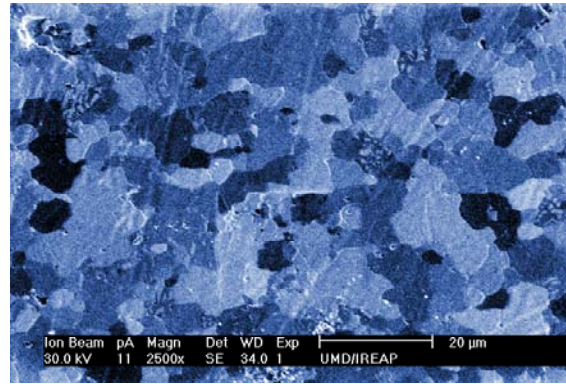


Figure 5: Image of sintered tungsten surface showing multiple crystal faces. Average grain size is O(10µm).

MOMENTS-BASED FORMULATION

The development of an energy-dependent relaxation time coincides with efforts to develop a modified emission probability model to replace Eq. [1], in which the energy of an incident electron affects its transmission probability *T(E)* over (or through for high fields) a barrier. By using a distribution function approach, parallel and transverse momentum expectation values are ascertained, the former used to evaluate the photoemission current, the latter to evaluate emittance (and both to evaluate brightness). Define the *n*th moment

$$M_n(x) = (2\pi)^{-3} \left(\frac{2m}{h^2}\right)^{3/2} \int_0^\infty E^{1/2} dE \times \int_0^{\pi/2} \sin \theta d\theta \left(\frac{2m}{h^2} Ex^2\right)^{n/2} T \left\{ (E + h\omega) \cos^2 \theta \right\} \times f_\lambda(\cos \theta, E + h\omega) f_{FD}(E) \left\{ 1 - f_{FD}(E + h\omega) \right\} \quad [8]$$

where $x = \cos(\theta)$ for parallel, and $\sin(\theta)$ for transverse components. *T* is the transmission probability; *f_λ* is the integrand of *F_λ*, and the factor *f_{FD}*(1-*f_{FD}*) represents the probability that the initial state is occupied and the final state is not based on the Fermi Dirac distribution. The revised relaxation times are used in the determination of the *f_λ* factor. The inclusion of the transmission probability factor, and the impact on the integration limits it entails, generally results in current density estimates on the order of 30% less than the Modified Fowler-Dubridge approach, all other factors being equal. Methods to calculate Eq. [8] numerically rely on approximations to the transmission probability and models for the relaxation time in the scattering factor: below, however, an asymptotic case is considered so as to provide a simple model of emittance and brightness.

Under the Richardson approximation for the transmission coefficient and the zero-temperature approximation for the FD functions, the asymptotic expressions for the transverse ($x = \sin\theta$) moments are [x]

$$M_0 \approx \frac{1}{(2\pi)^2} \left[\frac{2m}{\hbar^2} \right]^{3/2} \frac{\mu^{1/2} (\hbar\omega - \phi)^2}{4(\mu + \phi)[p(\hbar\omega + \mu) + 1]} \quad [9]$$

$$M_2 \approx \frac{2m\mu(\hbar\omega - \phi)}{3\hbar^2(\hbar\omega + \mu)} M_0$$

From the definition of the emittance [xi] as

$$\varepsilon_{n,rms}(z) = \frac{\hbar}{mc} \sqrt{\langle x^2 \rangle \langle k_x^2 \rangle - \langle xk_x \rangle^2} \quad [10]$$

and following a derivation and approximations (uniform emission over a circular uniformly illuminated surface area) analogous to that leading to the widely-used thermal emittance relation

$$\varepsilon_{n,rms}(therm) = \rho_c / (4\beta_T mc^2)^{1/2} \quad [11]$$

where ρ_c is the cathode radius and β_T is $1/k_B T$, it can be shown that $\varepsilon_{n,rms}(photo)$ is proportional to the illumination radius and the root of the 2nd and 0th moments, or

$$\varepsilon_{n,rms}(photo) \approx \frac{\rho_c}{2} \left[\frac{\mu(\hbar\omega - \phi)}{3mc^2(\hbar\omega + \mu)} \right]^{1/2} \quad [12]$$

$$\frac{B_n}{(1-R)I_\lambda A} \approx \frac{3qmc^2}{2\pi^2 \mu^3 \hbar\omega} \left(\frac{(\hbar\omega + \mu)(\hbar\omega - \phi)}{1 + p(\mu + \hbar\omega)} \right)$$

where B_n is the brightness [xii], R is the reflectivity, I_λ is the laser intensity per unit area, and A is the illuminated area. The brightness ratio in Eq. [12] is designed to forestall issues associated with reflectivity, laser particulars, and illumination area. Two observations are important: first, the emittance does not depend on the scattering factor to leading order (the brightness does through the p factor); second, the asymptotic form of B_n indicates that an optimal wavelength exists for which the brightness is maximized. The behavior of $\varepsilon_{n,rms}$ and B_n are shown in Figure 6.

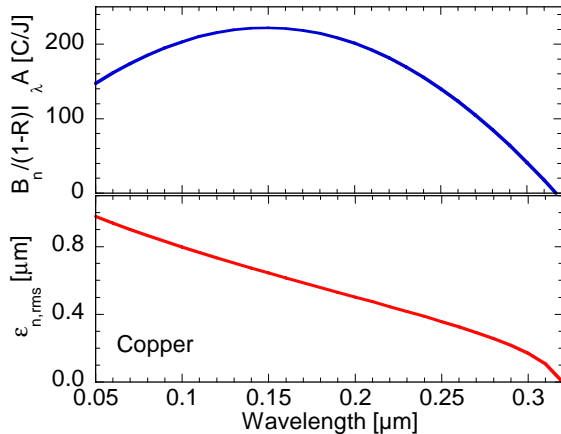


Figure 6: emittance and brightness ratio as a function of incident laser wavelength for copper parameters for conditions described in Ref. [viii].

Experimental values of emittance at 233 nm are approximately 50% larger than the theoretical value shown. The emittance of thermionic sources are generally within a factor of 2 larger than the theoretical

estimate entailed by Eq. [11], and it is reasonable to presume similar explanations hold here: non-linear field components in the cavity, wakefields, non-uniformity of the illumination source (laser), thermal effects, quantum efficiency non-uniformity due to contamination or cathode structure, and space-charge effects occur for sufficiently high charge in the bunch, and likely some combination contribute to the theoretical-experimental differences between the simple asymptotic limit herein and experiment.

CONCLUSION

We have presented a revised photoemission model to account for theoretical-based scattering models and a moments-based approach for the evaluation of quantum efficiency. The revised scattering model enabled good agreement with experimental data of cesiated surfaces. The moments-based approach allowed for simple asymptotic expressions of emittance and brightness.

Acknowledgements

We gratefully acknowledge funding provided by the *Joint Technology Office* and the *Office of Naval Research*. In addition, we have benefited from interaction with many colleagues: in particular we thank (*alph*) C. Bohn, C. Brau, D. Dimitrov, D. Dowell, Y.Y. Lau, J. Lewellen, E. Nelson, J. Petillo, and J. Smedley.

REFERENCES

- i K. L. Jensen, Donald W. Feldman, Nathan A. Moody, and Patrick G. O'Shea, *Journal of Applied Physics* **99**, 124905 (2006).
- ii J. J. Petillo, E. M. Nelson, J. F. DeFord, N. J. Dionne, B. Levush, *IEEE Trans. El. Dev.* **52**, 742 (2005).
- iii D. A. Dimitrov, D. L. Bruhwiler, J. R. Cary, P. Messmer, P. Stoltz, K. L. Jensen, D. W. Feldman, P. G. O'Shea, *Conference Proceedings of the 27th Intl. Free Electron Laser Conference* (Stanford, CA, Aug. 21-25, 2005), paper TUPPE039.
- iv A. V. Lugovskoy, Igor Bray, *J. Phys. D: Appl. Phys.* **31** L78 (1998).
- v Harald Ibach, Hans Lüth, *Solid State Physics 2nd Ed.*, (Springer-Verlag, Berlin, 1995).
- vi F. Ladstädter, U. Hohenester, P. Puschnig, C. Ambrosch-Draxl, *Phys. Rev.* **B70**, 235125 (2004)
- vii N. A. Moody, D. W. Feldman, P. G. O'Shea, K. L. Jensen, J. L. Shaw, J. E. Yater, (*Free Electron Laser Conference*, Berlin, Aug 27-Sep 1, 2006)
- viii D. H. Dowell, F. K. King, R. E. Kirby, J. F. Schmerge, J. M. Smedley, *Phys. Rev. Spec. Top.-AB* **9**, 063502 (2006)
- ix Data from J. M. Smedley (*private communication*).
- x K. L. Jensen, P. G. O'Shea, D. W. Feldman, N. A. Moody (*submitted to Appl. Phys. Letters*)
- xi Patrick G. O'Shea, *Phys. Rev.* **E57**, 1801 (1998).
- xii C. Brau, *Nucl. Inst. Meth. Phys. Res.* **A407**, 1 (1998).